**Supporting Information**

# Influence of dissolved silicate on rates of Fe(II) oxidation

Andrew S. Kinsela, Adele M. Jones, Mark W. Bligh, An Ninh Pham, Richard N. Collins,
Jennifer J. Harrison, Kerry L. Wilsher, Timothy E. Payne, T. David Waite

## Contents

## Major ion composition of Little Forest trench water at time of sampling

**Table S1**: Major ion composition of the Little Forest Legacy Site trench water at the time of sampling (29/1/16).

| Cation[1] | Concentration (mg/L) | Anion[2] | Concentration (mg/L) |
|---|---|---|---|
| Al | 0.08 (<0.01) | $Br^-$ | 0.34 (<0.01) |
| Ca | 1.59 (<0.005) | $Cl^-$ | 18.8 (<0.01) |
| Fe | 57.2 (<0.01) | $F^-$ | 0.08 (<0.01) |
| K | 1.01 (0.01) | | |
| Mg | 2.95 (<0.001) | Alkalinity[3] | Concentration (mg/L) |
| Mn | 0.117 (<0.001) | $HCO_3^{2-}$ | 80.52 |
| Na | 21.2 (0.013) | | |
| P | 0.4 (<0.05) | Organic C[4] | Concentration (mg/L) |
| S | 0.16 (<0.1) | DOC | 5.8 |
| Si | 15.8 (<0.1) | | |
| Actinides[5] | Activity (Bq/L) | Other[6] | |
| $Pu^{239+240}$ | 30.4 – 45.6 | pH | 6.60 |
| $Am^{241}$ | 15.7 – 27.8 | ORP | +150 mV (SHE) |

[1] Cations were measured by a combination of ICP-OES and ICP-MS using standard methods (detection limits in brackets)

[2] Anions were determined by IC using standard methods

[3] Bicarbonate concentration was determined by alkalinity titration

[4] Dissolved organic carbon concentration was determined by combustion catalytic oxidation

[5] Actinides were separated onto various resin cartridges before being analyzed by alpha spectrometry, as detailed by Harrison et al.[1]. Values represent a range of activities previously measured on site (Apr to Jun 2015)

[6] Other chemical parameters were determined using a hand-held logging instrument connected to a flow-cell continuously pumping water from the trench

## Further Methodology Details

### Lepidocrocite and silica-ferrihydrite synthesis methods

Lepidocrocite was formed following the method of Cornell and Schwertmann[2], with minor modifications, as follows. Lepidocrocite was precipitated by oxidation of a 0.05 M $FeCl_2.4H_2O$ solution at pH 6.4 to 6.8. Oxidation was achieved by constant bubbling with a vacuum pump supplying ~5 L $min^{-1}$ of air to the solution. The pH was maintained by the constant addition of 0.5 M HCl. Bubbling was maintained until the pH stabilized.

Ferrihydrite (2-line) was formed following the method of Cornell and Schwertmann[2] without modification, as follows. 1 M KOH was added to 0.1 M $Fe(NO_3)_3.9H_2O$ to rapidly increase the pH to between 7 and 8. Addition of KOH was such that the pH never exceeded pH 8.

Silica-ferrihydrite was formed following the method of Jones et al.[3] without modification. A 0.01 M $NaSiO_3$ solution was adjusted to pH 3 with concentrated $HNO_3$, to which $Fe(NO_3)_3.9H_2O$ was added to obtain a final concentration of 0.01 M. 1M KOH was then added until the final pH had stabilized between pH 7 and 8.

### X-ray absorption spectroscopy beamline set up

Transmission measurements were made over the energy range 6914 to 7862 eV with the beam sourced from a 1.9 T wiggler. Beam energy was selected using a double-crystal fixed-exit Si(111) monochromator, fully tuned with a rhodium-coated toroidal mirror. Sample transformation was prevented by maintaining at ~5 K with a closed-cycle He cryostat (CRYO Industries of America). A thin foil of elemental Fe was analyzed simultaneously to normalize energy shifts.

**Fe(II) oxidation kinetics for synthetic and environmental Fe(II) solutions (0.0179 mM)**

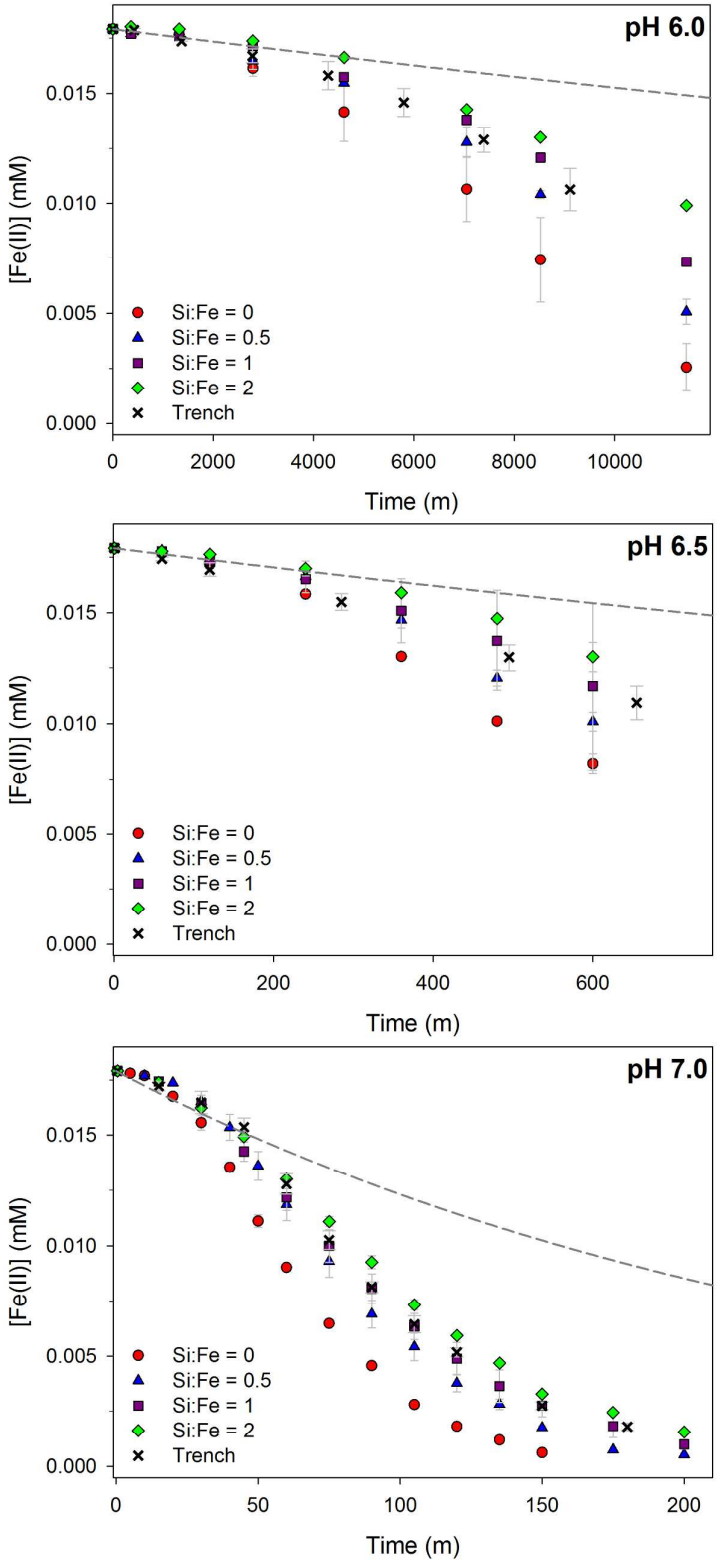


**Figure S1**: Oxidation of 0.0179 mM Fe(II) from trench and synthetic solutions at pH 6.0 (top), 6.5 (middle) and 7.0 (bottom) in the absence and presence of dissolved silica (data points). Error bars are standard deviations of triplicates. Dashed grey lines represent published homogeneous Fe(II) oxidation rates.

## Thermodynamic calculations of trench water Fe(II) speciation

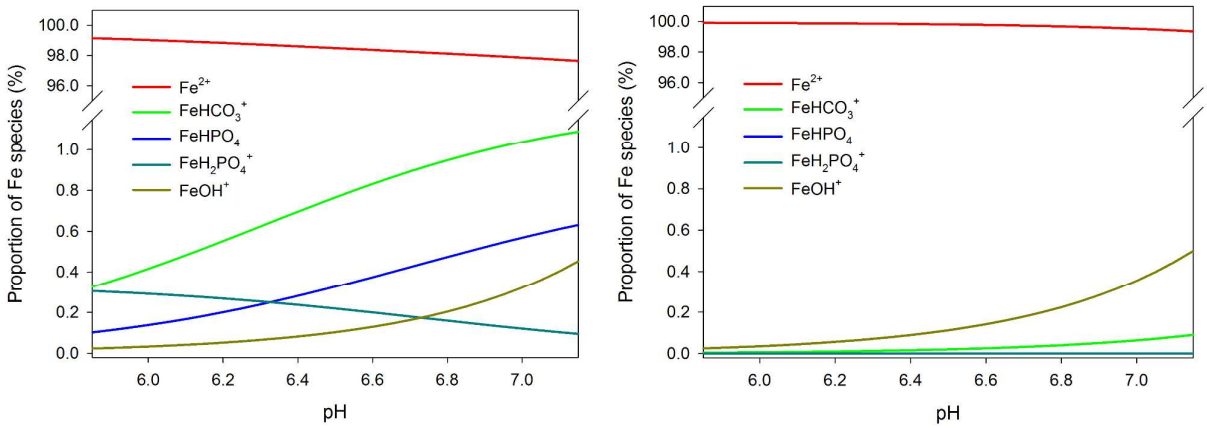


**Figure S2**: Thermodynamic calculations showing the proportions of Fe(II) species in trench waters using the parameters listed in Table S1 (left) and the synthetic solutions (right). Note the break in y-axes values to distinguish species of lower concentrations.

## FTIR spectra of Fe(III) oxidation products conducted at pH 6 and 6.5

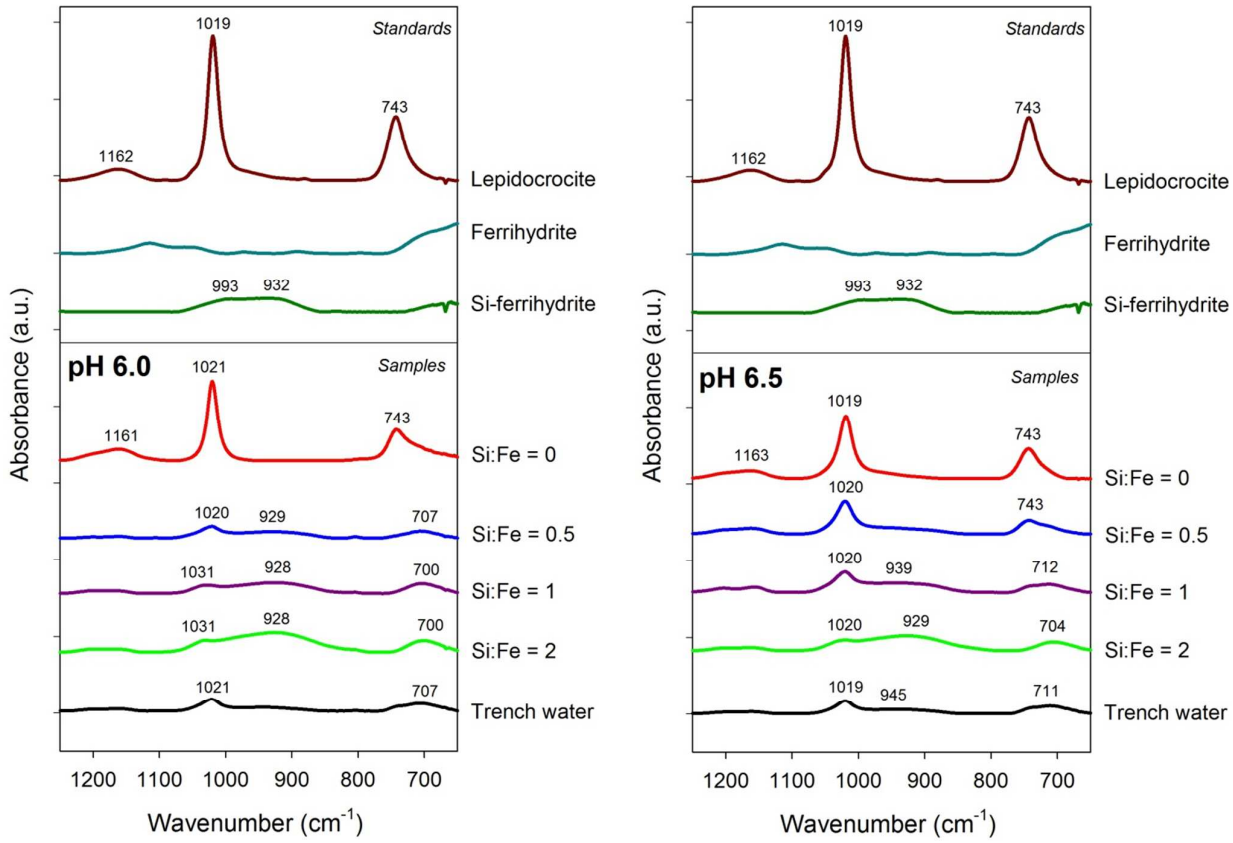


**Figure S3**: FTIR spectra for Fe(II) oxidation solid-phase products derived from trench and synthetic waters in the absence and presence of silica at varying molar ratios, at pH 6.0 and 6.5.

## XAS spectra of Fe(III) oxidation products conducted at pH 6.5 and 7

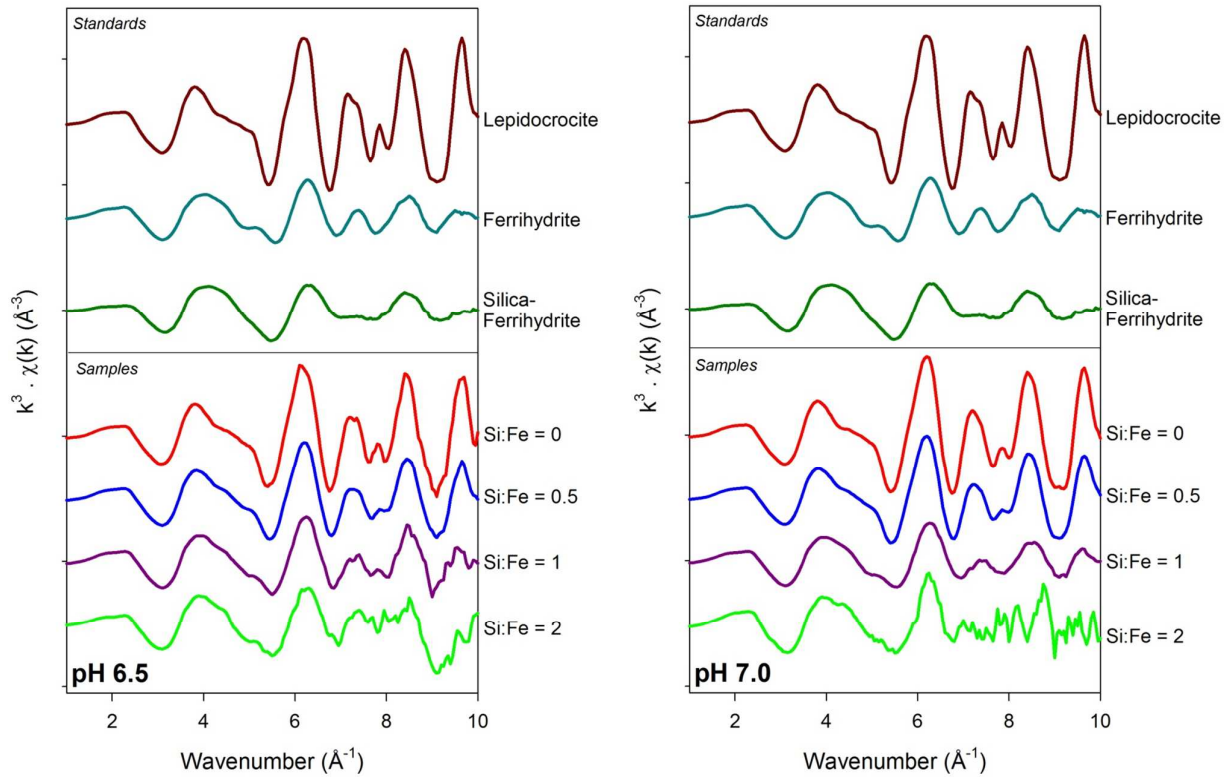


**Figure S4**: XAS spectra for Fe(II) oxidation solid-phase products in the absence and presence of silica at varying Si:Fe molar ratios, at pH 6.5 (left) and pH 7 (right).

As shown in Figure S4 (and reflected by LCF fits in Table 1), lepidocrocite was found to occur when solution ratios of Si:Fe = 0.5 were used, in contrast to the findings of Voegelin et al.[4]. One possible reason for this difference may be due to enhanced Si-polymerization occurring during our reaction experiments. No pH manipulation of the Si-stock solution was made prior to its addition to the reaction flasks with the pH being ~ 11-12. Although it is unlikely that Si-polymerization would have occurred prior to its addition, this may have occurred during Fe(II) oxidation (when pH was between 6 and 7) thereby limiting the effect of Si on Fe(III) polymerization and favoring lepidocrocite formation. Alternatively, the vigorous washing procedure, post Fe(II) oxidation, may have contributed to a disproportionate removal of the more reactive silica-ferrihydrite over lepidocrocite.

## Fe(II) sorption to Fe(III) oxides lepidocrocite and silica-ferrihydrite as a function of pH (Si:Fe = 0)

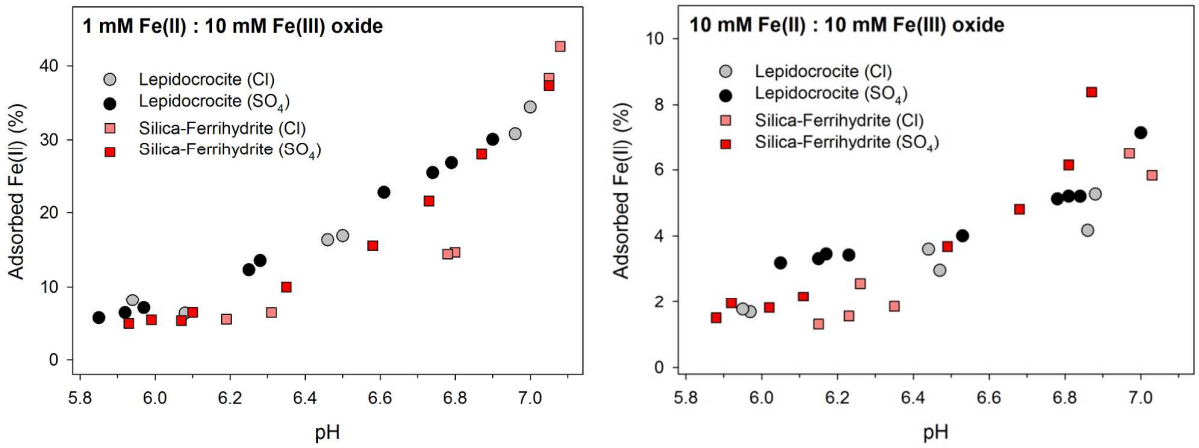


**Figure S5**: Adsorption of Fe(II) to lepidocrocite and silica-ferrihydrite as a function of pH in the absence of dissolved silicate; normalized to Fe(III) content at molar ratio of 1:10 (left) and 1:1 (right) Fe(II):Fe(III).

## Extent of Fe(II) sorption to Fe(III) oxides in the presence of dissolved silicate (Si:Fe = 1; Si:Fe = 2)

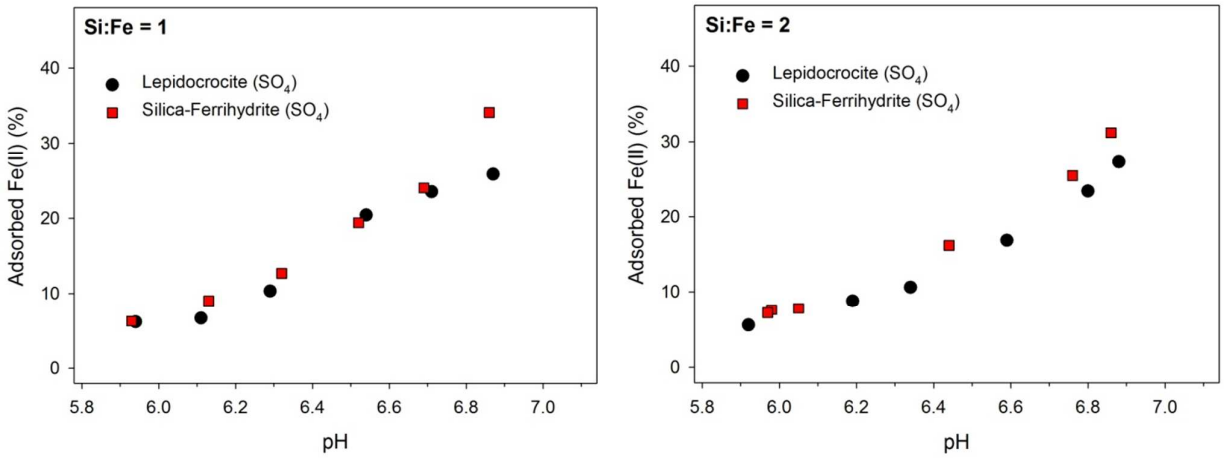


**Figure S6**: Adsorption of Fe(II) to both lepidocrocite and silica-ferrihydrite as a function of pH; normalized to Fe(III) content at ratios of 1:10 Fe(II):Fe(III), and at Si:Fe ratios of 1 (left) and 2 (right).

## Further information on the kinetic modeling: foundations and underlying assumptions

**Table S2**: Kinetic model and rate constants used to account for the oxidation behavior of Fe(II) in the presence of $O_2$ and dissolved silicate.

| # | Reaction | | $k$ ($M^{-1}$ $s^{-1}$) | | |
|---|---|---|---|---|---|
| | | | **pH 6** | **pH 6.5** | **pH 7** |
| 1 | $Fe^{II} + O_2 \rightarrow Fe^{III} + O_2^-$ | Homogeneous Fe(II) oxidation | 1.1E-03 [a] | 3.5E-03 [a] | 2.7E-01 [b] |
| 2 | $Fe^{III} + Fe^{III} \rightarrow LEP + LEP$ | LEP precipitation | 1.0E+05 [c] | 5.0E+05 [c] | 1.0E+06 [c] |
| 3(+)$^{\alpha}$ | $Fe^{II} + LEP \rightarrow Fe^{II}$-LEP | Adsorption of Fe(II) to LEP (formation) | | 1.0E+08 | |
| 3(-)$^{\alpha}$ | $Fe^{II} + LEP \leftarrow Fe^{II}$-LEP | Adsorption of Fe(II) to LEP (dissociation) | 2.0E+04 | 4.2E+03 | 2.3E+03 |
| 4 | $Fe^{II}$-LEP + $O_2 \rightarrow$ LEP + LEPi | Heterogeneous Fe(II) oxidation on LEP | 4.96 | 80.2 | 88.7 |
| 5(+)$^{\alpha}$ | $Fe^{III} + Si \rightarrow Fe^{III}Si$ | Fe(III) and silicate complexation | | 1.0E+08 | |
| 5(-)$^{\alpha}$ | $Fe^{III} + Si \leftarrow Fe^{III}Si$ | Fe(III) and silicate complexation | | 1.2E+03 | |
| 6 | $Fe^{III}Si + Fe^{III}Si \rightarrow$ SiFHY + SiFHY | SiFHY precipitation | 2.5E+04 | 3.5E+04 | 1.0E+05 |
| 7(+)$^{\alpha}$ | $Fe^{II}$ + SiFHY $\rightarrow$ $Fe^{II}$-SiFHY | Adsorption of Fe(II) to SiFHY (formation) | | 1.0E+07 | |
| 7(-)$^{\alpha}$ | $Fe^{II}$ + SiFHY $\leftarrow$ $Fe^{II}$-SiFHY | Adsorption of Fe(II) to SiFHY (dissociation) | 4.0E+04 | 5.3E+03 | 3.0E+03 |
| 8 | $Fe^{II}$-SiFHY + $O_2 \rightarrow$ SiFHY + SiFHYi | Heterogeneous Fe(II) oxidation on SiFHY | 0.8 | 48.6 | 58.4 |

Notes: LEP = lepidocrocite, LEPi = internalized / non-reactive lepidocrocite
SiFHY = silica ferrihydrite, SiFHYi = internalized / non-reactive silica ferrihydrite
[a] King[5], [b] Pham and Waite[6]
[c] Values from Pham et al.[7] were used as a starting point and constrained to within one order of magnitude.
[α] Reactions (#3, #5 and #7) where equilibrium has been assumed
All other values fitted from data collected in this study

The kinetic model shown in Table S2 was constructed by including the minimum number of reactions thought necessary to adequately describe the oxidation of Fe(II) in the absence (reactions #1 to #4) and in the presence (reactions #1, #5 to #8) of dissolved silicate.

Treatment of a solid phase that is simultaneously undergoing formation and participating in reactions is highly problematic in a chemical kinetic model. In order to preserve a simple set of reactions that both reflect the key processes and maintain mass balance we have chosen to treat the Fe(III) atoms that comprise the solid assemblage as individual entities. For example, Fe(III) atoms of lepidocrocite are represented as LEP if they are external and accessible for reaction with dissolved species or as LEPi if they are internal and inaccessible. In this way the amount of solid phase is simply quantified and partitioned into reactive and unreactive components. While in reality reactive sites on a solid phase do not correlate directly with individual atoms, the quantities are linked and reasonably proportional. Other possible approaches to this problem such as particle population modeling lead to intractable complexity and the requirement to assign values to properties such as reactive surface area to mass ratio and surface reactive site density.

Before discussing individual reactions, collectively, the model parameters were fit by using published data (e.g. homogeneous rate constants) as fixed, unchangeable values. This was followed by using rational assumptions of rate constants based on published data of a similar nature (e.g. solid-phase formation rate constants, heterogeneous Fe(II) oxidation rate constants) as starting points and constraining these values to be within an order of magnitude of published values. Rate constants for the remaining reactions were then assigned based on

a knowledge of the relative rates of those processes compared to published values. All Si:Fe data within each pH value were fitted simultaneously.

The rate constants for **Reaction #1** have been established previously by King[5] and Pham and Waite[6] across the pH range 6 to 7. These rate constants were determined at low micromolar to nanomolar concentrations where Fe(III) solid phases were absent.

The values for **Reaction #2** were interpreted from data supplied in Pham et al.[7]. Pham et al.[7] in Table 2 identified Fe(III) formation constants at pH 6, 6.5 and 7 as being 0.43, 1.29 and 3.78 x $10^6$ $M^{-1}s^{-1}$. These values were used as starting points in our kinetic model, and during the manual fitting process these constants were allowed to vary within one order of magnitude. Our calculated constants provided in Table S2 are well within one order of magnitude difference from Pham et al.[7], and importantly trend accordingly with pH as per described by Pham et al.[7].

We recognize that this is a very simplistic representation of what is a complex series of processes, involving the hydrolysis of Fe(III), the formation of polymers which then form primary particles which are subsequently subject to aggregation processes in the formation of flocs. Due to both the complexity (in terms of the number of additional reactions required) and uncertainty (of assigning any rate constants) surrounding these processes they were simplified to Reaction #2, which represents a single (total) dissolved Fe(III) entity forming a single reactive site on a solid (LEP). This approach was chosen because it 1) captures the second order dependence on Fe(III) concentration, 2) produces a basic entity that is able to partake in subsequent reactions such as adsorption, and 3) maintains mass balance.

**Reaction #3(+)**, the formation/forward reaction depicting the adsorption of Fe(II) to lepidocrocite was assumed to be very fast and therefore, when combined with the reverse reaction, effectively achieved instantaneous equilibrium, as has been proposed previously by Tamura et al.[8, 9]. Since we have depicted the reactants as a dissolved Fe(II) species and a solid phase entity LEP, the product comprises both these components as a complex.

**Reaction #3(-)**, the reverse desorption / dissociation reaction was partly constrained by the results of the Fe(II) adsorption measurements (Figure 4), which displayed increasing adsorption with increasing pH. As such, the rate constants were set at similarly proportioned values, reflecting the lower levels of adsorption measured at more acidic pH values. The empirical adsorption studies also revealed that this reaction rate is dependent on the inner-sphere Fe(II)-Fe(III) adsorption, rather than total Fe(II) adsorption. As this was shown to be markedly higher for lepidocrocite compared to silica-ferrihydrite, a faster set of reaction rates was assigned to lepidocrocite.

**Reaction #4**, the heterogeneous oxidation of Fe(II) adsorbed to lepidocrocite was depicted as a reaction between oxygen and the complex resulting from the adsorption reaction (#3(+)). Since heterogeneous oxidation is the likely mechanism of lepidocrocite crystal growth, the adsorbed Fe(II) atom is transformed to a LEP entity, and the original LEP component of the complex becomes internalized in the crystal structure (represented as LEPi). In this way only Fe(III) atoms located on the surface of the solid phase are accessible for further reaction.

The scientific literature is sparser with regards to silica ferrihydrite formation. As no previous identification has been made for Fe(II)-silicate species, only the Fe(III)-silicate phase was considered for any complexation reactions. With the reported large stability constant for $FeHSiO_3$ (log k = 22.7)[10], the assumption of a 1.0E+08 formation rate constant for **Reaction #5(+)** is justified. It is important to note that this species will completely dominate (>99%) dissolved Fe(III) speciation even at the lowest silicate concentration.

Similarly, the rate of silica ferrihydrite precipitation (**Reaction #6**) had to be estimated. It was assumed to be slower than that reported previously for lepidocrocite (approximately one order of magnitude), and increased

with pH. As shown in Figure S7 below, the analyses indicated that this parameter had minimal sensitivity on Fe(II) oxidation, and therefore could be considered a sensible value.

As with **Reaction #3$_f$** above, the formation/forward reaction depicting the adsorption of Fe(II) to silica ferrihydrite (**Reaction #7(+)**) was also assumed to be fast. The reverse desorption / dissociation reaction (**Reaction #7(-)**) was also constrained between pH values by the empirical adsorption measurements.

Again, similar to **Reaction #4** the oxidation of Fe(II)-adsorbed on silica ferrihydrite (**Reaction #8**) was described as the reaction of the adsorption complex producing a reactive and an unreactive solid phase entity.

**Importance of each reaction (from Table 1) upon the oxidation of 0.0895mM Fe(II) at pH 6.0, 6.5 and 7.0**

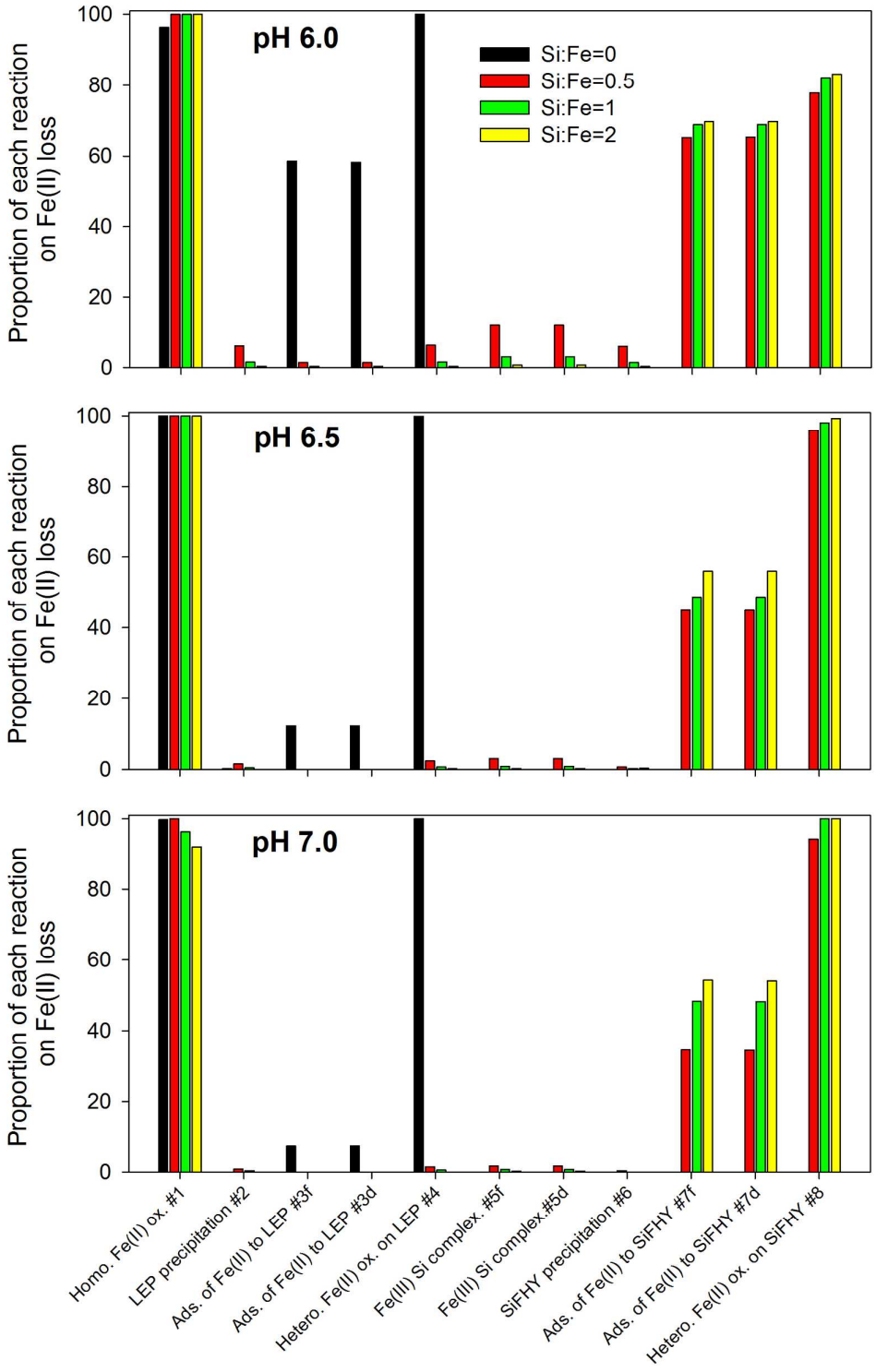


**Figure S7**: Relative importance of each reaction (#1 to #5 from Table 1) upon the oxidation of 0.0895mM Fe(II) at pH 6.0, 6.5 and 7.0. Values were calculated at the approximate mid-points of all reactions when Fe(II) oxidation rates were at their fastest and normalized to the fastest reaction for each Si:Fe ratio.

## Zeta potential values (pH 6 to 7) of lepidocrocite and silica-ferrihydrite in the presence of dissolved silicate

Zeta potential measurements were made on the two reference materials lepidocrocite and silica-ferrihydrite using dynamic laser scattering (Malvern Zetasizer). The washed reference materials (as described previously) were resuspended to give an Fe(III) concentration of 1 mM. Silicate was added to the suspension in molar ratios of 0, 0.5, 1 and 2, and the pH adjusted to 6.0, 6.5 and 7.0 before being thoroughly mixed. A 1 mL aliquot was then transferred to a capillary cell for DLS analysis.

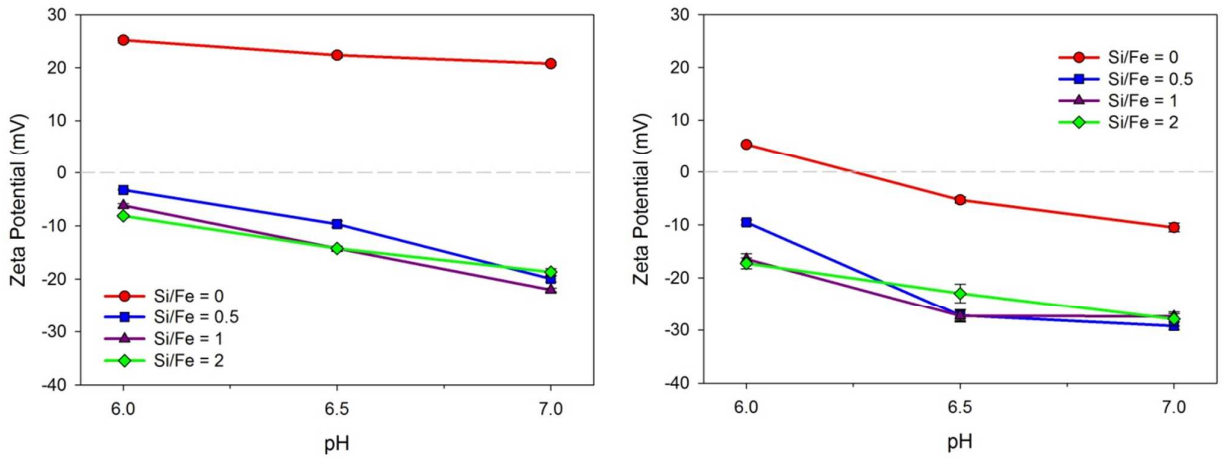


**Figure S8**: Zeta potential measurements across the pH 6 to 7 for lepidocrocite (left) and silica-ferrihydrite (right) under varying molar ratios of silicate and iron(III).

## References


1. Harrison, J. J.; Zawadzki, A.; Chisari, R.; Wong, H. K. Y., Separation and measurement of thorium, plutonium, americium, uranium and strontium in environmental matrices. *Journal of Environmental Radioactivity* **2011,** *102*, (10), 896-900.
2. Cornell, R. M.; Schwertmann, U., *The iron oxides: Structure, properties, reactions, occurences and uses*. Wiley-VCH: Weinheim, 2003.
3. Jones, A. M.; Collins, R. N.; Rose, J.; Waite, T. D., The effect of silica and natural organic matter on the Fe(II)-catalysed transformation and reactivity of Fe(III) minerals. *Geochim. Cosmochim. Acta* **2009,** *73*, (15), 4409-4422.
4. Voegelin, A.; Kaegi, R.; Frommer, J.; Vantelon, D.; Hug, S. J., Effect of phosphate, silicate, and Ca on Fe(III)-precipitates formed in aerated Fe(II)- and As(III)-containing water studied by X-ray absorption spectroscopy. *Geochim. Cosmochim. Acta* **2010,** *74*, (1), 164-186.
5. King, D. W., Role of carbonate speciation on the oxidation rate of Fe(II) in aquatic systems. *Environmental Science and Technology* **1998,** *32*, (19), 2997-3003.
6. Pham, A. N.; Waite, T. D., Oxygenation of Fe(II) in natural waters revisited: Kinetic modeling approaches, rate constant estimation and the importance of various reaction pathways. *Geochim. Cosmochim. Acta* **2008,** *72*, (15), 3616-3630.
7. Pham, A. N.; Rose, A. L.; Feitz, A. J.; Waite, T. D., Kinetics of Fe(III) precipitation in aqueous solutions at pH 6.0-9.5 and 25°C. *Geochim. Cosmochim. Acta* **2006,** *70*, (3), 640-650.
8. Tamura, H.; Goto, K.; Nagayama, M., The effect of ferric hydroxide on the oxygenation of ferrous ions in neutral solutions. *Corrosion Science* **1976,** *16*, (4), 197-207.
9. Tamura, H.; Kawamura, S.; Hagayama, M., Acceleration of the oxidation of $Fe^{2+}$ ions by Fe(III)-oxyhydroxides. *Corrosion Science* **1980,** *20*, (8-9), 963-971.
10. Morel, F. M. M.; Hering, J. G., *Principles and applications of aquatic chemistry*. John Wiley & Sons: USA, 1993.